

# Turbine Technical Design Report

2024 Collegiate Wind Competition

University of Wisconsin-Madison



**Overall Team Lead:** Josh Delgado ([jdelgado22@wisc.edu](mailto:jdelgado22@wisc.edu))

**Team Advisor:** Scott Williams ([spwilliams@wisc.edu](mailto:spwilliams@wisc.edu))

**Faculty/Staff Advisors:** Randy Jackson, Jennifer Franck

<u>Electrical Team Lead:</u> Nazrie Hasan ( <a href="mailto:mbhasan@wisc.edu">mbhasan@wisc.edu</a> )	<u>Mechanical Team Lead:</u> Robert Miller ( <a href="mailto:rjmiller@wisc.edu">rjmiller@wisc.edu</a> )	<u>Aerodynamics Team Lead:</u> Vinaayak Puliyadi ( <a href="mailto:vpuliyadi@wisc.edu">vpuliyadi@wisc.edu</a> )	<u>Substructure Team Lead:</u> Mark Kuzel ( <a href="mailto:mkuzel@wisc.edu">mkuzel@wisc.edu</a> )
--	---	---	--

## Table of Contents

Executive Summary .....	2
Design Objective .....	2
Mechanical Design & Analysis .....	3
Generator Assembly .....	3
Pitch Control .....	4
Base Plate, Bearing Blocks, Bearings, and Drive Shaft .....	5
Aerodynamic Design and Analysis .....	6
Blades Design .....	7
Blade Manufacturing .....	7
Blade Simulation and Testing .....	7
Nacelle Design and Manufacturing.....	8
Substructure Design and Analysis.....	8
Design Selection and Analysis.....	9
Manufacturing and Installation .....	10
Electrical Systems .....	10
Generator.....	10
Turbine Electronics .....	10
Load Electronics .....	11
Variable Load System.....	12
Start State .....	13
Normal Operation State .....	13
Rated Power State .....	13
Emergency Stop State.....	14
Load Disconnect State .....	14
Turbine Assembly .....	14
Commissioning Checklist .....	15
References: .....	16

## **Executive Summary**

This design report outlines the technical design, manufacturing, and testing of the University of Wisconsin-Madison WiscWind competition team's scale wind turbine created for the 2024 Collegiate Wind Competition. The team has redesigned all mechanical components, electrical systems, and code for this year's competition to maximize available points in all testing categories.

The main priority of the mechanical sub-team was to improve the safety and durability of the generator component after a failure that resulted in the team forfeiting all turbine performance points, besides substructure, in the prior year. The mechanical sub-team utilized an innovative screw assembly approach that allows for complete control of the position of the rotors with respect to the stator at all times. The team then focused on optimizing other components to improve overall turbine function and efficiency. These components included designing and manufacturing a custom pitch control system, made specifically for the needs of the turbine and blade assembly, and redesigning all bearing blocks and baseplates to increase the aerodynamic efficiency from last year's design.

The aerodynamics sub-team's priorities this year involved extensive analysis and design in Qblade. The team worked to combine different types of airfoils together to design a blade that would have optimized power output during the middle wind speeds (6 m/s – 9 m/s) relative to other standard airfoils. After some instances of blades breaking due to rotational speeds or contact during travel or installation, the team analyzed different methods of manufacturing.

The substructure team's main goals were to improve on key deficiencies from previous year's design. These included the time to install the substructure, the total weight, and the maximum torque the substructure could sustain. The team tested two finalized designs in a new testing cell which utilized a pulley and weights system in order to achieve consistency for all torque measurements.

The main focus of the electrical team this year is to redesign the whole electrical system by reducing the complexity and improving it based on the data from last year. To achieve this, the team designed a new Axial Flux Permanent Magnet Synchronous Generator based on last year's knowledge. In addition, the team also designed PCB for the turbine and load electronics. This is a major improvement from last year as we learned to design the sub-system ourselves such as the relay modules, communication system and load switching board. The team utilized new sensors and microcontrollers for the system and rewrote the code to accommodate all the changes.

## **Design Objective**

WiscWind's design objective for the 2024 Collegiate Wind Competition was to design and manufacture a small-scale offshore wind turbine to fulfill all the turbine testing tasks. To successfully achieve the power curve performance task, our team designed a variable load system to maximize power output at each wind speed based on the RPM reading from the hall effect sensor. Next, the team designed a new communication system that utilized UART protocol to ensure a reliable exchange of data between turbine and load enclosure in fulfilling all tasks. To make sure the team maintains stable power during the *Control of Rated Power* task, we used a PI controller to actively pitch the blades from 11m/s to 15m/s using linear actuators. For the Safety task, our team utilized a current and voltage sensor to detect load discontinuity to make sure the system stopped the turbine. The substructure was designed to engage the sand in the sand-water tank, over last year's design which involved adding counterweights. This was accomplished by creating a box design with angled plates that could all slide directly into the sand. Additionally, the box design allows for a fast installation and has a high failure torque.

Another part of the design objectives was to not reuse any component. No components are being reused for this year's competition except for the DC2465A Evaluation Board Rectifier. The team decided to reuse the same rectifier that utilized 3 LT4320 controllers and 6 N-Channel FETs because the component was purchased as an investment to be used for multiple years. After extensive research was done by the team this year to find a new rectifier, the team determined that there was no active rectifier

that is more efficient than DC2465A in the market currently. An alternative active rectifier was attempted to be manufactured by the team, however the efficiency loss was too great, resulting in the team deciding to reuse this component.

## **Mechanical Design & Analysis**

### **Generator Assembly**

The generator for this wind turbine was designed, manufactured, and assembled in-house. The magnetic field was maximized for current generation, using 24 magnets with 25.4 mm diameter, 6.35 mm thickness, and 4623 gauss magnetic flux density. Twelve radially patterned magnets were aligned and secured to rotors assembled on both sides of a printed circuit board (PCB) stator. When the magnetic rotors rotate near the circuit board, current is generated. The rotors were water jet cut from  $\frac{1}{8}$ " thick, 4140 alloy steel. A PLA-printed part was placed around the magnets to increase the surface area available to secure the magnets to the rotor with JB weld. This is necessary because each magnet pulls with 120 N of force when the two rotors are located a minimal distance apart. A 6 mm distance is ideal to produce maximum current and accommodate the 2.3 mm thick stator.

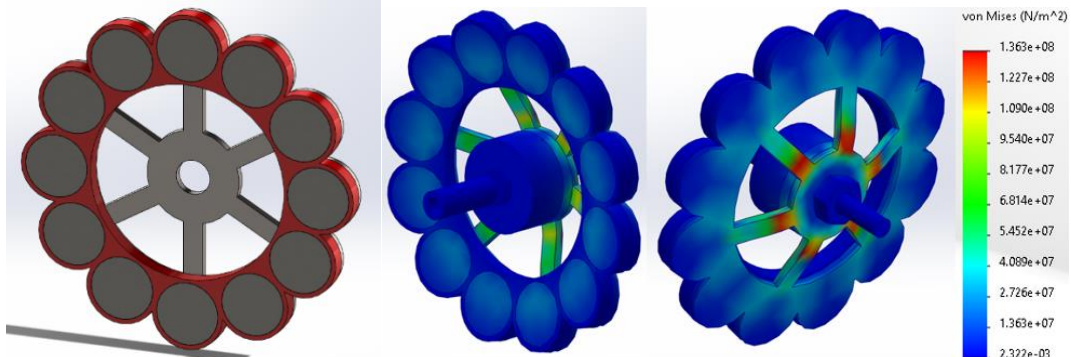


**Figure 1.** Image of the rotor with assemble PLA magnet holder and magnets (left) and FEA stress analysis on rotor(right)

Because the rotors pull toward each other with a total of 1.44 kN of force, rotor deformation was a major concern. Because of these large forces, 4140 alloy steel was chosen, boasting a yield strength of roughly 824 MPa. Using this material allowed for the mass MOI optimization for each rotor to 618 kg-mm<sup>2</sup> while mitigating the deformation concern. Shown in Figure 1, an FEA of the rotor assembly on the shaft displayed maximum stresses of 135.1 MPa at the locations in red when the maximum magnetic forces are experienced. This is well below the yield stress and will ensure that the rotors do not deform during assembly or turbine rotation.

The generator shaft, shown in Figure 2, is coupled to the drive shaft and used to translate rotational energy from the shaft into the rotors. The shaft assembly features a large shoulder in the center for the rotors to rest upon, minimizing the bending moment experienced by weak sections of the rotors. The shaft assembly also features threading on either side of the shoulder to secure the rotors from sliding axially, and from rotating independently of the shaft.

The most important feature of the generator shaft is its ability to assemble the generator together in a timely, but controlled manner. Because of the large forces that the rotors apply to each other, it is impossible and dangerous for a human to assemble it by hand. The shaft shown in Figure 2 features a large, 12 mm diameter rear half and a smaller, 8 mm diameter front half. The rear shaft has a tightly toleranced, 8 mm hole in its center to accept a locator pin slightly smaller than 8 mm in diameter from the front half. When rotors are assembled to each half of the shaft with an M10x1.25mm nut, the shaft halves

are brought together with the locator pin placed into the rear shaft. The M8 bolt in the rear shaft is slowly turned and the halves are brought together in a controlled manner, preventing any rotor damage or safety issues.

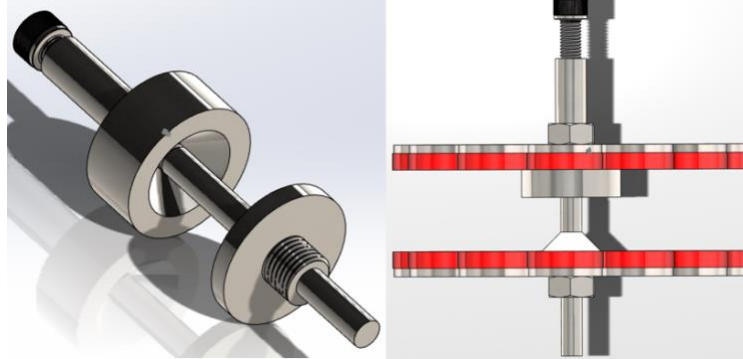


**Figure 2.**

The left image displays the front and rear half of the shaft coming together. The right image displays the generator shaft with rotors attached.

To ensure that the threading is strong enough for this screwing mechanism, and to ensure that the shaft will not magnetically attract the rotors, the shaft was machined from 304 stainless steel. This steel provides a tensile yield strength of roughly 215 MPa and a shear yield strength of roughly 124.7 MPa. Using a grade 12.9 bolt, the threads of the shaft are the limiting factor for failure. The shear stress on the threads is 5.6 MPa and the normal stress is 8.4 MPa, providing a safety factor of 22 and 25 respectively. This means that thread stripping failure should not be a concern, even with repeated use.

## Pitch Control

To achieve maximum turbine efficiency, blade orientation relative to wind speed must be achievable. This is done by decoupling the movement of the blade's orientation from the spinning of the turbine generator. The pitch control mechanism works similarly to modern helicopter blade control designs where mechanical linkage and bearings are used to move the pitch control actuator off the spinning blade assembly so it does not contribute to rotational inertia.

Figure 3 shows the full 3D CAD model of the pitch control mechanism on the left, and the sectioned view with only one strut and one blade connector is included for visibility. Blades connect by being inserted into the blade connector by a 6mm shaft protruding out the end of the blade. The blade shaft has a hole that allows a screw to pass through both the blade connector and blade shaft to lock the rotation of the blade and blade connector. The blade connector can rotate 100 degrees around the upper strut bearing and is articulated via the transfer strut. The transfer strut then connects to the lower strut bearing which connects to the inner decoupler housing. All the aforementioned components spin with the blades and contribute to the rotational inertia. To decrease the rotational inertia and increase accuracy in pitch orientation, the component's weight and rigidity have been optimized.

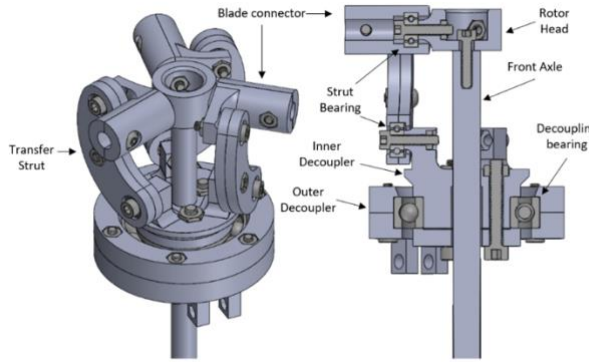


**Figure 3.** Pitch control mechanism (left) sectioned view without patterning (right)

The decoupling bearing decouples the outer decoupler housing from the rotation of the inner decoupler housing. From this point on, none of the components contribute to the rotational inertia and have been optimized for robustness instead of weight. The outer decoupler housing attaches to the linear actuator, which drives the entire decoupling housing back and forth. Decoupling the linear actuator from the rotation of the generator significantly reduces the rotational inertia and complexity of the system.

Shown in Figure 4, an FEA on the pitch control mechanism ensures that it can handle stresses from the aforementioned 0.336 N-m maximum torque, and 7.3 N thrust force. A 70 N axial force was also tested to ensure that the maximum setting of the linear actuator would not break the system, though a much smaller force will be applied during operation. Tests with the real, built mechanism displayed similarly positive results.

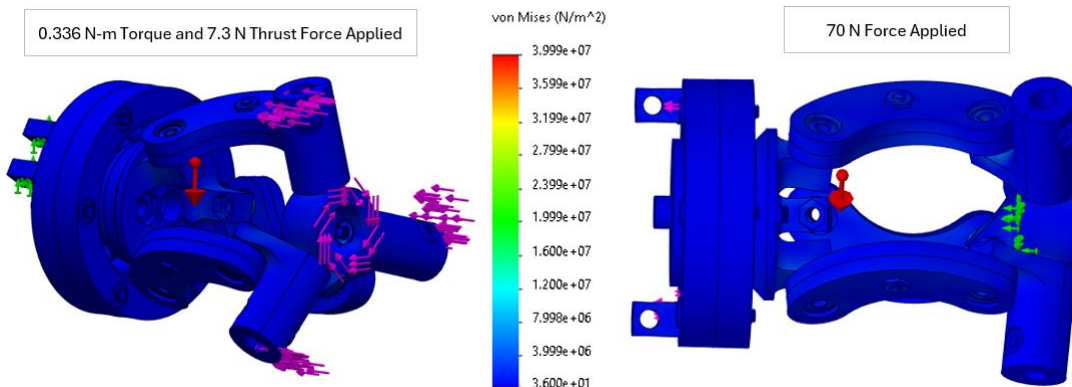


**Figure 4.** An FEA shows the effect of gravity, a 0.336 N-m torque, a 7.3 N thrust force, and a maximum 70 N linear actuator force on the pitch control mechanism

## Base Plate, Bearing Blocks, Bearings, and Drive Shaft

The base plate is laser cut from  $\frac{3}{8}$ " thick 6061 aluminum material. The base plate is intended to hold the bearing blocks and stator holder on the top side and fasten to the support shaft with the substructure on the bottom side. As seen in Figure 5, the base plate is small relative to the entire wind turbine assembly. This is intended to bring the vertical, front-bearing block support farther back from the turbine blades. When wind travels through the blades and hits the front surface of the bearing block, disruption in the flow occurs, and turbulent vortices and eddies are created. If the blades are close to the front bearing block and interact with those vortices and eddies, the blade rotation will be hindered.

Reducing the surface area directly behind the blades is necessary to mitigate this effect, so the vertical support of the front bearing block was moved backward.

As shown in Figure 5, a longer bearing block with a sloped vertical support accommodates the shorter base plate. The front bearing block contains two bearings, one at the rear and one in the front, and slots to secure a linear actuator for the pitch control mechanism. Printed from a PLA material, the front bearing block is fastened to the base plate using M6x1.00mm bolts and nuts. Because this part supports a gravitational force of 4.5N from the pitch control mechanism and blades, and a maximum thrust force of 7.5N during rotation, there is no concern of failure from this part. The moment of the pitch control mechanism and blades at the front of the bearing block is also offset by the moment of the generator components at its rear. At the rear, a bearing block made of the same PLA material is used. It is also fastened with M6x1.00mm bolts and nuts, and because this part sees only a gravitational force from the generator components, there is no risk of failure. This block location was also made adjustable to accommodate the variation in the fabrication and assembly of the generator components.

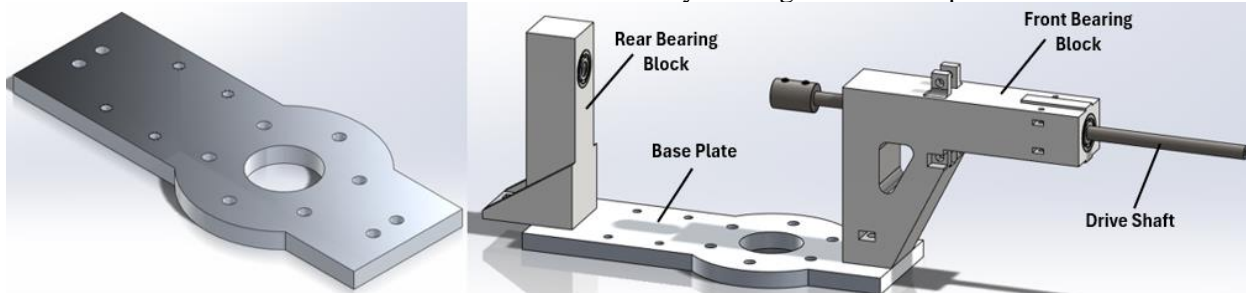


**Figure 5.** A CAD image of the base plate(left) and a CAD image with bearing blocks, bearings, drive shaft, and coupling (right)

The drive shaft at the front of the wind turbine is supported by bearings in the front bearing block. This is an 8 mm, 12L14 carbon steel shaft, and it was purchased from McMaster for its easy machinability and low cost. With a yield strength of 415 MPa, 12L14 is strong enough to handle the maximum torsional load of 0.336 N·m applied by the generator for braking. Utilizing SolidWorks FEA analysis, this shaft achieves a safety factor of ~66. While a smaller shaft could have met the stress requirements, this shaft was cheap and made assembly much easier.

For seamless rotation, radial ball bearings with an 8 mm internal bore and 22 mm outer diameter were purchased from McMaster. Because the radial and thrust forces seen by these bearings from the component weight, blade thrust, and blade drag are very small, failure was not the primary consideration. The total revolutions for the life of the bearing were calculated based on the turbine spinning at 2500 rpm for 365 days straight, resulting in 1.314e09 revolutions. The fatigue safety factor for all three bearings was calculated utilizing maximum bearing capacities found on McMaster-Carr, and a reliability of 99%. The results of these calculations are found in Table 1 below. In the end, these bearings were selected for their compatibility with our shaft diameter, and their minimal outer diameters. By having small bearing outer diameters, the bearing blocks were made narrower, improving aerodynamics.

**Table 1.** Safety factors and calculated loads experienced by each bearing.

Bearing	Load [N]	Safety Factor
Rear	5.987	76.03
Center	7.571	70.28
Front	4.951	80.33

## Aerodynamic Design and Analysis

## Blades Design

Airfoil selection was a critical part of the design process for the blades. Due to the small scale of the wind turbine blade and low wind speeds, the wind turbine operates at low Reynolds numbers where laminar separation effects can severely degrade the performance of airfoils not designed for this regime [1]. Furthermore, large-scale wind turbine blades have multiple airfoils situated throughout the blade, with larger airfoils located at the root and smaller airfoils located near the tip. The SG 6040 series airfoils were used due to their focus on lower Reynolds Number flow and use in hybrid blades [1].

The SG 6040 and 6043 airfoils were chosen as the root and primary airfoils, respectively. The 6040 was designed to be used as a root airfoil and the 6043 was optimized for lower Reynold's number flows [1]. The hybrid blade designed by the team, seen in Figure 6, was designed to have a higher power output at middle wind speeds to take advantage of the point weighting of the competition. The blade uses the SG 6040 airfoil from the base to the midpoint, where it transitions to the SG 6043. The 6040 is a larger root airfoil optimized for the lower velocities closer to the base of the blade, allowing it to be more effective than a primary airfoil in that region. The 6043 is a smaller primary airfoil optimized for the higher velocities near the tip of the blade. Different configurations with both airfoils were simulated but it was found that keeping the transition point at the midpoint worked best for the competition wind speed range.

The team used QBlade to model the wind turbine blades. This software uses the Lifting Line Free Vortex Wake Method [2] for its calculations/simulations. The process to create blades in QBlade involved slicing blades into 20-50 cross-sections. The team utilized QBlade's built-in optimization tool design the blades for a desired tip-speed ratio. Inputting a desired tip-speed ratio would automatically adjust the blade's twist and taper. Once blades are modeled in QBlade, simulations and wind tunnel testing can be performed. This Qblade simulation provided the given power coefficient, shown in Figure 6, illustrated the power coefficient for various tip speed ratios. While the optimal power coefficient occurs when the tip-speed ratio is around 3, a tip-speed ratio of 3.5 was chosen as the blade size at a tip-speed ratio of 3 was too large and resulted in the inertia of the turbine being too high which affected the turbine performance.

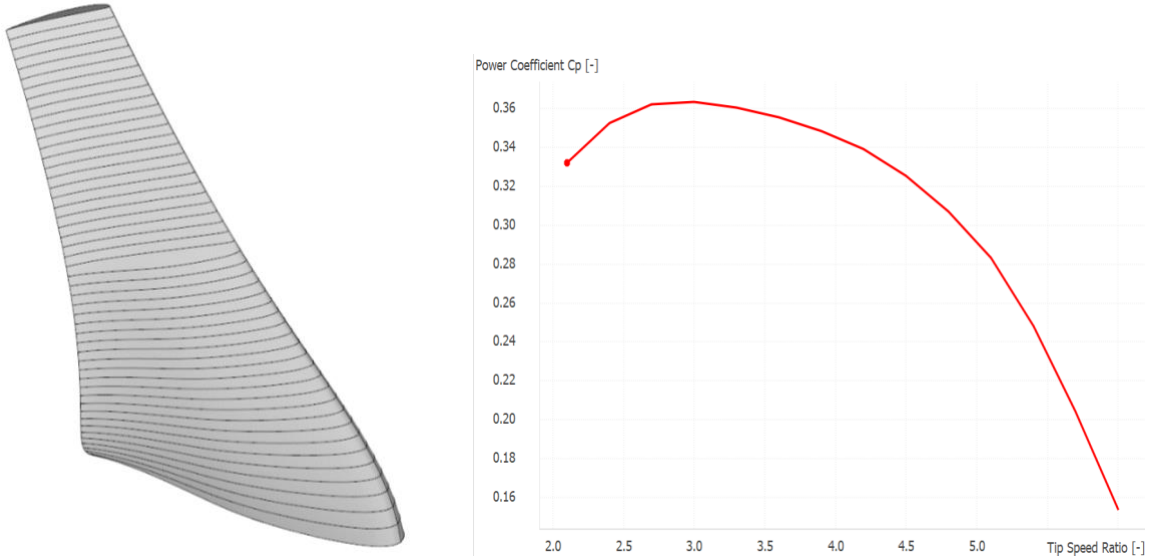


**Figure 6.** Chosen SG 6040-6043 Combined Airfoil Blade (left) and Cp-Lambda Report (right)

## Blade Simulation and Testing

The simulation tool in QBlade allowed the team to produce theoretical results for each blade design. Simulations provided important information about potential blade designs without needing to spend excess time manufacturing, validating, and testing each new design. A simulation could be set up by establishing the input parameters, including air density, air viscosity, and wind speed. Next, the range of tip-speed ratios to vary for the blades would be specified. This defined the simulation, which could then output graphs for desired variables, such as coefficient of power, thrust, or torque. This could then be repeated for different wind speeds to get a better profile of the blade's performance.

Once blades were modeled, simulated, and manufactured, they could move on to real-world testing with the use of a wind tunnel. Several types of wind turbine blades were tested including the combined SG 6040 and SG 6043, Wortmann FX 60-126, and SG 6040. These blades were tested at the wind speed range of 5 m/s to 11 m/s. The results of the test are shown in Figure 7 for each blade demonstrating wind speed vs tested power.

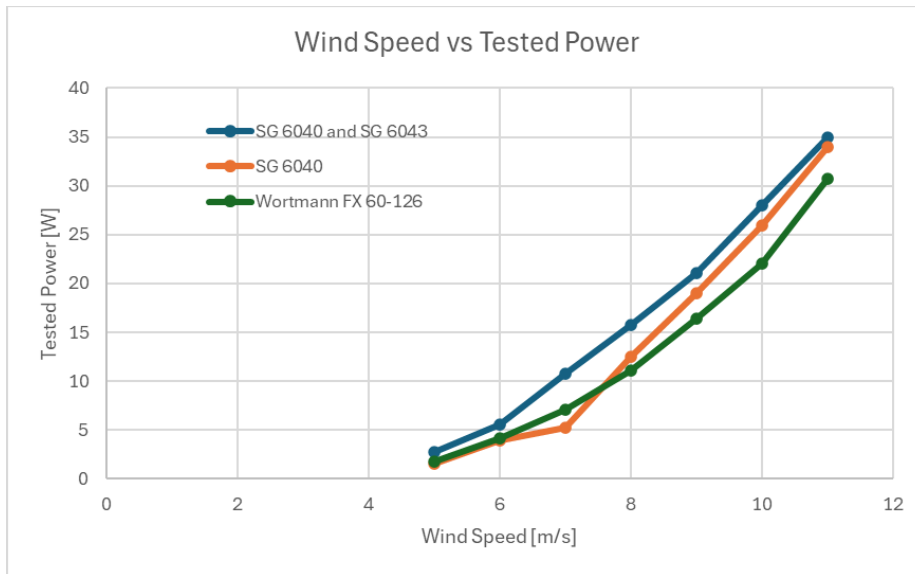


**Figure 7.** Power vs Wind Speed for various wind turbine blades

## Nacelle Design and Manufacturing

The aerodynamics team also focused on developing a nacelle for the turbine. The main purpose of this is to reduce the drag force on the turbine. There are two main types of drag forces to limit: pressure-induced drag and viscous friction drag. Pressure-induced drag is proportional to frontal surface area while viscous friction drag is proportional to total surface area. The nacelle needs to be as aerodynamic and as small as possible to achieve this. To measure these drag values, two non-dimensional values will be calculated: the coefficient of friction (.0129) and the coefficient of drag (.083). These values were found through SolidWorks Flow Simulation, as the nacelle was designed using SolidWorks.

The nacelle was manufactured via 3D printing using PLA. To fully 3D-print the Nacelle in the Ultimaker S5 Printer, it was split into four sections and is easily removable to access the inner workings of the turbine at any moment, as seen in Figure 15. It was printed with small (5mm diameter, 2mm thickness) holes for magnets to be glued into the nacelle for easy assembly.

## Substructure Design and Analysis

The primary goal of the substructure team this year was to improve in key areas of struggle from the previous year's design. This included resistance to tipping due to high incipient wind speed, increased ease and speed of installation, and an overall reduction in weight compared to last year. To quantify the maximum torque experienced by the turbine during tipping, a drag force equation was utilized to calculate the force experienced by the turbine at the maximum wind speed of 22 meters per second. When considering the swept rotor diameter and the pipe as the projected areas, the torque induced by the wind was found to be approximately 48 N-m. This calculation served as the primary design criteria for which all manufactured structures would be evaluated against.

## Design Selection and Analysis

Utilizing a design matrix developed in the fall semester, the team decided upon two primary designs that would be manufactured and tested. The two designs selected were an interlinking cross-plate design and a box design which utilized angled plates. Both designs utilized angular plates, which utilized the inherent resistance to tipping provided by the sand. As the substructure attempted to tip, the large surface areas of these plates would severely restrict the movement of the nearby sand, significantly increasing the overall strength of the design. The two proposed designs can be seen below in Figures 8 and 9.

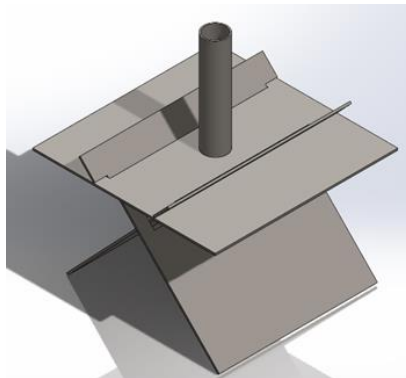


**Figure 8.** Cross Plates SOLIDWORKS Design

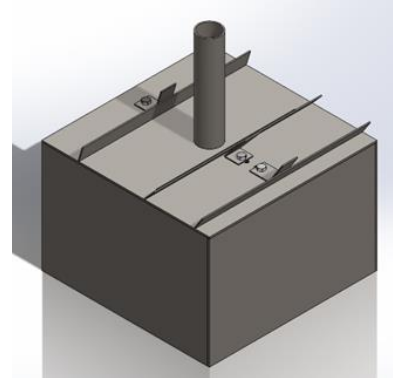


**Figure 9.** Final Box SOLIDWORKS Design

Both designs were tested on three primary criteria, which were integral to success. These criteria were installation time, total weight, and maximum induced torque before tipping. To do this, a new testing setup was created. Using a 30" x 20" x 15" storage container, several bags of sand, and water, the team recreated the testing cell utilized at the competition. To simulate the torque experienced by the substructure due to oncoming winds, a pulley system was purchased and had weights attached to represent the drag force due to varying wind speeds. This change improved the consistency of our data as the previous year's testing involved pulling a force sensor and reading the output weight once the substructure began to tip, which did not clearly indicate the exact torque required in order to tip the substructure.

**Table 3.** Testing Data for Failure Torques, Weights, and Installation Times for Primary Designs

	Failure Torque [N·m]	Average Installation Time [minutes]	Weight [kg]
Cross-Plate Design	44	8	5.8
Box Design	70	3	10

From these results, we found that while the cross-plate design significantly reduced weight, the box design partially sacrificed weight for significant improvements to the factor of safety for the substructure and the installation speed. The adherence to more of our design criteria finalized our decision to move forward with the box design.

## Manufacturing and Installation

The developed substructures utilized a variety of manufacturing methods. Both designs required the use of waterjet cutting to manufacture the baseplate and angled side plates. This was due to the precision and affordability provided by waterjet cutting compared to other methods such as laser cutting. Furthermore, the added precision allowed for the precise tolerancing of the slots for the side plates, as multiple widths which varied by millimeters were utilized to install the side plates at varying angles. For both designs, a connecting stem was welded to the top baseplate to provide a path for the electrical cable through the stem. To ease the installation process of the angled side plates into the baseplate, small pieces of sheet metal were waterjet cut, bent, and screwed into place on top of the baseplate. Long slits were cut into the baseplate to allow for the lateral adjustment of these guides in order to provide the easiest possible installation for the baseplates.



Figure 10. Cross Plates Manufactured Design



Figure 11. Final Box Design chosen for competition

## Electrical Systems

### Generator

The team designed a new PCB stator this year to increase the back EMF constant ( $k_e$ ), by adding the number of turns in the stator. The  $k_e$  is calculated using this equation:

$$K_e = \frac{(\sqrt{2} \cdot N_s \cdot N_m \cdot N_t \cdot A_m \cdot B_{gap})}{\pi} \quad [1]$$

where  $N_s$  is the number of coils in series,  $N_m$  is the number of magnetic poles,  $N_t$  is the number of turns per coil,  $A_m$  is the area of magnet face, and  $B_{gap}$  is the magnetic flux density.

This will help the turbine to produce voltage at lower wind speeds and increase the overall turbine efficiency at high wind speeds. Although increasing the EMF constant increases the voltage output, it has been verified through testing that the maximum output voltage at 11 m/s is 28V, which will remain below the competition limit of 48V. The resistance of each phase also increased slightly due to the increased number of turns. However, the increment is not that significant due to heavy and thick copper traces chosen for the winding on the PCB stator. The phase resistance has been calculated and verified to be  $0.67\Omega$  per phase.

### Turbine Electronics

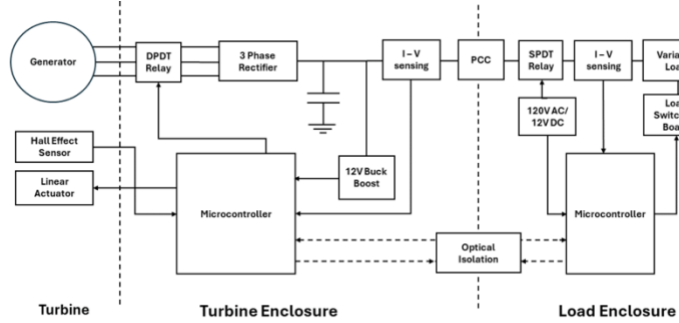


**Figure 12.** One Line Diagram Electrical System

The electronic design this year was created with simplicity and efficiency in mind. Firstly, the 3-phase power will pass through a 12V DPDT electromechanical relay that will be shorted during the emergency stop state. Then, this AC voltage will be rectified using a 3 phase AC/DC Rectifier. This rectified voltage will be filtered through a smoothing capacitor to reduce the ripple voltage following the imposed competition rule to produce stable power between  $\pm 10\%$  of the maximum average power. This filtered voltage will then pass through a 12V DC/DC Buck Boost converter to produce a stable 12V DC rail to power the Arduino UNO R4, two L12 Actuonix actuators, and the previously mentioned DPDT relay. The LM5118 Evaluation Board 12V Buck Boost converter was chosen for its wide input range from 5V-75V DC which boasts a high frequency from 85-95% by using the voltage input from the generator's output voltage. This 12V rail will be coupled with a 10mF resistor to power the system during the *Load Disconnect State*. This will give an adequate time for the linear actuator to feather the blades to stop the turbine from spinning. The total amount of energy storage in the turbine electronics is 7.155 Joules.

Last year, the team used a pitot tube along with an analog differential pressure sensor to measure wind speed as the sole input data for the control algorithm. However, the sensor did not produce consistent wind speed data during wind tunnel testing due to ground proximity and air turbulence. It is crucial for the team to get reliable data because this will be used to determine the combination of parallel resistors used in the load enclosure and for the active pitch control during the *Rated Power State*. Therefore, the team decided to use the A3144 hall effect to measure the shaft RPM due to its reliability in producing precise and consistent data. This sensor will output a pulse when it detects the south pole of the magnets on the rotor. The team wrote the code in Arduino IDE from scratch to sense the number of pulses per revolution, and these numbers will then be calculated to get the shaft RPM. Next, the Adafruit INA260 current & voltage sensor is used to continuously monitor the voltage in the PCC rail to help in achieving the *Safety Task* by comparing the current voltage to the threshold voltage needed to enter *Load Disconnect State*. All the sensors in the turbine electronics are being powered by the 5V output of the microcontroller.

These RPM, voltage and current values will then be transmitted to the load electronics through the new microcontrollers. Arduino UNO R4 is chosen as the microcontroller for the system as it has hardware serial ports on the board that allows the team to transition swiftly from wireless communication to wired by utilizing UART Serial Protocol. Due to changes in the communication protocol, all the codes were written from scratch and the practice helped the team to better understand the low-level overview of two-way communication system. To minimize the complexity of this transition, the team used ACPL-772L optocouplers, which boast high speed data transfer and positive logic truth table. These optocouplers are connected through RJ45 cable that ensures the communication line is optically isolated and optimal data transfer between both microcontrollers.

## Load Electronics

One of the most significant changes compared to last year's design is the new streamlined load system. To achieve that, the team took initiative to design two PCBs for the entire load system in Altium. The first PCB consists of a 12V SPDT relay, an optocoupler, an Adafruit INA260 sensor, and the Arduino UNO R4. This reduced the complexity of the system from last year by removing the 5V buck converter in the circuit that used to power the 5V SPDT relay module. The second PCB consists of 8 N-Channel MOSFETs to realize the variable load system that is inspired by one previously designed by John Hopkins University. This PCB will then be connected through wires to the parallel combination of resistors placed on the aluminum plate to help with heat dissipation. To further help the dissipation of heat, a 22 CFM exhaust outlet fan is located on the wall of the load enclosure.

## Variable Load System



**Figure 13.** Variable Load Switching PCB

The team designed the variable load system by utilizing 8-N Channel MOSFETs as switches that adjust the parallel combination of load resistances with respect to the RPM value received from the turbine microcontroller. To calculate these resistance values, we first calculated the theoretical power input from the blades. Next, we calculated the shaft speed by utilizing the torque value of the blades and the wind-swept area from 5 m/s to 11 m/s which will be translated to RPM. Next, the RPM values are used to calculate the AC voltage of the generator by multiplying it with the machine constant and converted to DC voltage. This voltage helps us to calculate the DC current and required resistance needed to maximize the power output. The team utilized Microsoft Excel to do the load calculation for each blade variation and generator model. This software helped the team to determine the best specifications needed for the new generator and the best blade for the competition.

The variable load system is designed with safety as the main priority. To protect the system from accidentally entering the *Load Disconnect State*, two resistors are coupled in series. These resistors then will be in parallel with the other 8 resistors when the MOSFETs' gates are turned on. The UNO R4 will output 5V to GPIO pins that are connected to the gates of MOSFETs to turn them on. Each gate of MOSFETs is paired with an LED in parallel to ease the process of verifying which gate is being turned on. This design helps to ensure a maximum resistance of  $40\ \Omega$  if the MOSFETs failed to turn on. As mentioned above, the optimal resistance values are different for each blade and generator. To facilitate the process of selecting the best combination of parallel resistance during testing based on the calculated values in Excel, the team developed a new JAVA code in IntelliJ that calculates the combination of resistors from the available power resistors that were purchased by the team in previous years. The code helped the team to reduce the time taken in figuring out the combination of parallel resistors and reducing the cost of buying more resistors. The code was developed to produce results with an accuracy of  $\pm 5\%$  with respect to the desired resistance value based on the RPM.

**Table 4.** Excel Variable Load Calculation Table

Input Torque (N-m)	RPM	Shaft Speed (Rad/s)	Peak Phase Voltage (V-LN)	DC Voltage Out (V)	Current Required (A)	Resistance Required	Generator Power (W)
6.26E-02	738.1258047	77.29632588	16.69600639	13.80759728	0.35044113	39.4006185	4.83875
1.01E-01	790.5458916	82.78574257	17.8817204	14.78818277	0.565408214	26.15487786	8.36136
1.41E-01	899.2277818	94.16687943	20.34004596	16.82121801	0.789332258	21.31069372	13.27753
0.177	1069.2799	111.9746893	24.18653288	20.00226269	0.990863899	20.18669034	19.81952
0.228	1181.918117	123.7701316	26.73434842	22.10930614	1.276367056	17.32205954	28.21959
0.309	1196.28933	125.2750809	27.05941748	22.37813825	1.729813247	12.93673654	38.71
0.336	1464.311546	153.3422917	33.121935	27.39184025	1.880961978	14.56267621	51.52301

## Turbine Control State Diagram

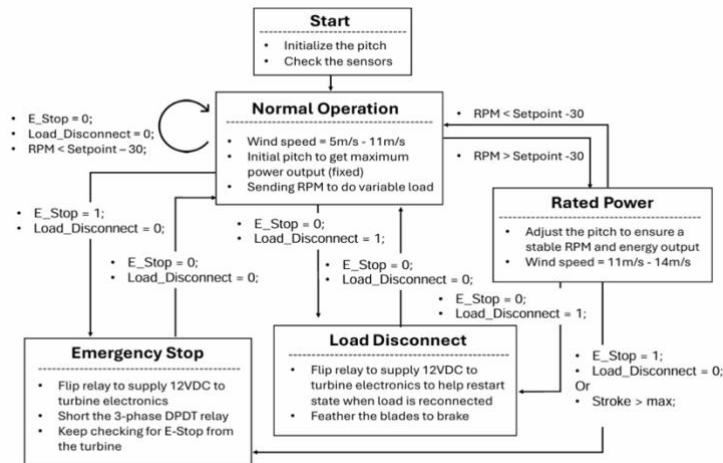


**Figure 14.** Turbine Control State Diagram annotated with required parameters to enter each state

### Start State

The start state initializes the pitch to an optimal position to encourage the turbine to spin at lower wind speed. The system will check data from each of the sensors to verify that the sensors work as intended. Once this check is completed, the turbine will proceed to *Normal Operation*.

### Normal Operation State

The blades will be feathered at a fixed position and the turbine electronics will read the shaft RPM from 5 m/s to 11 m/s and transmit the value to accordingly adjust the variable load in order to produce maximum power output. During this state, the turbine and load microcontrollers will keep checking the RPM, voltage, current reading and the E-Stop button to enter *Emergency Brake State* or *Load Disconnect State* based on the condition sets for each state.

### Rated Power State

In this state, the team decided to use PI control to maintain the RPM and the power output at 11 m/s. Our pitch control system for this state takes RPM as input and the stroke length of the actuator as the output. The load resistance is fixed in this state. This state is activated if the RPM is measured to be 30 rev/min lower than the RPM when wind speed is at 11m/s. After entering the state, the error between the set point and RPM the actual RPM will be calculated and put into the PI control calculator to obtain the length that needs to be adjusted for the actuator. The actuator will push the blades to the correct pitch angle to maintain the power output between 11m/s to 15 m/s. If the actual RPM is larger, the control system will push the blades forward to receive less effect from the wind and vice versa. In the case of the

microcontroller reads the actuator wants to pitch more than maximum value dedicated for it, the turbine will enter the *Emergency Stop State* to brake the turbine.

## **Emergency Stop State**

The system enters this state if the e-stop button is open to allow the turbine to shut down within 10 seconds to fulfill the *Safety Task*. This is achieved by shorting the 3-phase through flipping the switch of the DPDT relay. To make sure the DPDT relay maintain the switch position, this relay will be powered by the 12V supplied from the load enclosure through switching the SPDT relay in the load enclosure. To exit the state, the turbine microcontroller detects the e-stop button as close and transmit the signal to load side. The load microcontroller will then switch back the SPDT relay to allow the turbine to power the resistive load and to open the DPDT relay so the system will enter the *Normal State*.

## **Load Disconnect State**

The system enters this state if the load microcontroller reads zero current and RPM greater than 500. It will transmit a signal to the turbine as soon it detects the condition to feather the blade out by using the power from the capacitor bank in the turbine side to maintain speed below 10% of the maximum average speed within 10 seconds as the competition rule. The SPDT relay in load electronics will flip switch to readily supply 12V DC to the load electronics to help feather the blades to the initial position when the load is reconnected. To exit this state, the turbine microcontroller will read voltage greater than the threshold value and transmit signal to load electronics and enter the *Normal Operation*.

## **Turbine Assembly**

In Figures 15 and 17 below, the final SOLIDWORKS models of the turbine with and without the nacelle can be seen. The shaft is connected via couplers and secured between the two bearing blocks which are screwed into the baseplate. The rotors are secured with the new generator shaft, which is screwed into place in between the PCB stator holder. This holder is also screwed into the baseplate, and secures the stator with a series of screws along the perimeter of the PCB. The front bearing block couples with the baseplate and linear actuators which are screwed into place along the side of the front bearing block. The final baseplate model, shown in Figure 16, illustrated two linear actuators being mounted on either side of the front bearing block to reduce the torque and increase stability. Additionally, the blades are inserted via a new attachment system to the pitch control, which will provide stronger resistance to rotational inertia and possible breakage at high wind speeds.

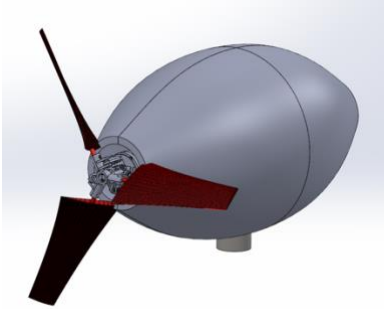


**Figure 15.** Turbine assembly in SOLIDWORKS with the nacelle



**Figure 16.** Turbine assembly without updated front bearing block

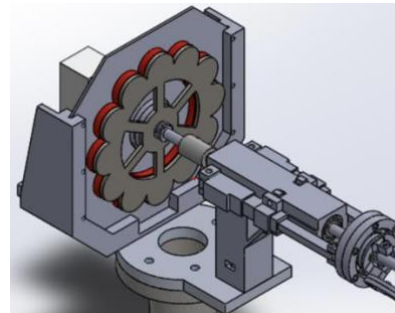


**Figure 17.** Final Turbine baseplate Assembly in SOLIDWORKS with updated front bearing block

## Commissioning Checklist

Step	Commissioning Task
#1	Insert main substructure box into the sand
#2	Slide in the angled side plates into the box using PVC and mallet method
#3	Use level to check that the baseplate is fully flush with the sand
#4	Run the power and signal cables through the foundation tubing while keeping the connectors out of water
#5	Connect the power and signal connector from the nacelle to their corresponding cable at the bottom of turbine tower
#6	Connect the power and signal connector from tower to the turbine enclosure
#7	Connect the DC output cable from the turbine enclosure to the PCC
#8	Connect the JST connectors from turbine enclosure to the PCC
#9	Connect the DC output cable from PCC to the input of load box
#10	Connect the RJ45 cable between turbine and load enclosure
#11	Connect the DC input cable from 12V power supply to the load box

#12	Plug the 120VAC to 12VDC power supply to the wall
#13	Plug the laptop to microcontrollers to verify all sensors and codes are working correctly
#14	Tighten all gland connectors and secure the electrical boxes

## References

[1] Giguere, P., & Selig, M. S. (1998, May). *New airfoils for small horizontal axis wind turbines*. New Airfoils for Small Horizontal Axis Wind Turbines. <https://m-selig.ae.illinois.edu/pubs/GiguereSelig-1998-JSEE-SG-NewAirfoils.pdf>

[2] Marten, D., Saverin, J., Behrens de Luna, R., & Perez-Becker, S. (n.d.). *Lifting line free vortex wake*. Lifting Line Free Vortex Wake.

[https://docs.qblade.org/src/theory/aerodynamics/lifting\\_line/lifting\\_line.html](https://docs.qblade.org/src/theory/aerodynamics/lifting_line/lifting_line.html)